Available online at www.sciencedirect.com

ScienceDirect

IFAC PapersOnline CONFERENCE PAPER ARCHIVE

IFAC PapersOnLine 54-4 (2021) 92–97

Stability of neural-network based train cruise advisory control with aperiodical measurements

A. K. Jain * **D. Berdjag** * **C. Fiter** ** **P. Polet** *

* *Université Polytechnique Hauts-de-France, CNRS UMR 8201, LAMIH laboratory, F59313 Valenciennes, France, (e-mail: AyushKumar.Jain@uphf.fr, Denis.Berdjag@uphf.fr Philippe.Polet@uphf.fr).*

** *CRISTAL, University of Lille, Lille, France, (e-mail: christophe.fiter@univ-lille.fr).*

Abstract: In this paper, a neural-network based driver advisory train cruise control system is considered. The controller assists the train driver with advisory signals by considering train and driver's actual state information (attention and fatigue) measured by dedicated sensors. Considering delays in sensor measurements, this paper aims to assess closed-loop stability of driver-in-the-loop advisory train cruise control. For this purpose, the driver model is considered as a time-varying system, the train model includes rolling and aerodynamic resistance forces and the advisory control is considered to be a sampled-data based three layer multi-layer perceptron. Further, the aperiodic measurement problem is approached as stability analysis of time-varying delayed system. Based on recent developments on the design of augemented Lyapunov Krasovskii Functional (LKF) using Bessel-Legendre inequality for time-varying delays, sufficiency conditions for the existence of L_2 stability of the driver-train system in terms of solvable Linear Matrix Inequalities are provided. Further a case study is presented to illustrate the effectiveness of the proposed method.

Keywords: Neural networks, Driver advisory system, Time-delay, LKF, Driver-in-the-loop, Human factors is vehicular systems.

1. INTRODUCTION

Train control systems (TCS) aim to assist and to some extent replace human driver for operational non-strategic tasks. In order to achieve/maintain desired performance/safety objectives, they not only require accurate train and driver models but also precise measurements. For example, the Automatic Train Operation (ATO) deals with almost all the control actions of the train operation. One of its task is real-time train speed control while following a reference trajectory. An effective ATO algorithm should not only track the desired position/velocity accurately, but also ensure energy saving, wear avoiding and comfortable driving actions. Due to legislative and certification issues regarding deployment of such fully autonomous ATO systems, semi-autonomous systems, i.e. driver-in-the-loop systems are gradually developed and implemented. The other key motive is to utilise existing rolling stock and to also gather enough operational data before massive deployment of full autonomous TCS. The current state of technology shows a plethora of certified assistance devices that supplement driver actions. The problem with these devices is that they are external to the ATO, which leads to time/energy/cost optimisation issues.

This article, while discussing train control system application, considers the general issues of deploying neural-network based advisory control i.e. two loop control cascade, with the internal loop controlled directly by the driver and the external loop controlled by a neural network, that we will call NNCDIL (Neural Network Control NNC with a driver-in-the-loop DIL). The motivation to use a NNC is straightforward: a neural network even in its simplest form of a three-layer fully connected feed-forward neural-network (TLFCFFNN) is capable to approximate advisory algorithms such as, Miglianico et al. (2018), with acceptable computational costs. This approach is called approximate computing, Mittal (2016), and is widely used for complex filter approximation, Chen and Wen (2019). Such network is to be trained offline, which is demanded by current industrial certification practices. The deployment of such NNCDIL systems, requires state of the art stability guarantees, and must consider practical exploitation constraints such as parameter variation of the DIL, both intra-driver (change of state during the mission) and inter-driver (different drivers for a train). Such issue can be solved by the use of external human sensing devices, based on cameras and biometric data Sikander and Anwar (2019). Currently available sensors suffer from some issues, such as relatively long processing times because of the need to process data over a time window that can be important (2-3 minutes for PERCLOS-based systems, Sommer and Golz (2010)) and because classification algorithms that might require variable time to converge. On top of these issues, the most challenging one is that such driver state measurements are uncertain, and some of the samples are to be discarded. Such discarded measurements breaks the periodicity in measurement updates, and can lead to stability issues, especially during inattentive state of the driver.

The main contribution of this article is the development of sufficient LMI-based stability criteria for such NNCDIL with aperiodically sampled driver measurements. Compared to our previous works, Jain et al. (2019), Jain et al. (2020a), Jain et al. (2020b), under LKF framework, we use the research presented

⋆ This work is supported by La Federation de Recherche Transports Terrestres & Mobilite (FRTTM 3733). An organization which is supported by The French National Center for Scientific Research (CNRS).

10.1016/j.ifacol.2021.10.016

in Park and Park (2018) about augemented LKF with Bessel-Legendre inequality, which is the current trend in control of time-delayed systems, Zhang et al. (2018), to precisely upper bound the derivative of an LKF. The framework presented in Park and Park (2018) is converted from time-varying delay to aperiodical sampling setting and used to derive sufficient L_2 stability conditions for the NNCDIL system, under driver state perturbation. The article is organised in four sections : Section 1 presents the motivation and the context of this research. Section 2 presents the problem statement and the models. The main contributions on stability criteria for NNCDIL is presented in Section 3. Further, Illustrative simulations are provided in Section 4. Finally, Section 5 concludes this article, and discusses future works. *Notations:* Throughout the article, $\mathbb{R}^n$, $\mathbb{R}^{n\times n}$ and $\mathbb{S}^n$ denote the sets of n-dimensional vectors, $n\times n$ matrices and symmetric matrices of $\mathbb{R}^{n\times n}$, respectively. The $\|.\|$ notation and the superscript 'T', stand for the euclidean norm and for matrix transposition, respectively. The set of positive definite matrices in $\mathbb{S}^n$ is denoted by $\mathbb{S}^n_+$. The notation $P \preccurlyeq 0$, with a matrix $P \in \mathbb{S}^n$ means that P is negative. $He\{A\} = A + A^T$. $diag\{\cdots\}$ and $col\{\ldots\}$ denote a block-diagonal matrix and a block-column vector, respectively. $Co\{p_1, p_2\}$ stands for a polytope generated by two vertices p_1 and p_2. The notation $\binom{l}{k}$ refers to binomial coefficients given by $\frac{l!}{((l-k)!k!}$. A symmetric term in a symmetric matrix is symbolised by a $'*'$.

2. PROBLEM SETTING

2.1 System Description

The driver advisory control system schematic represented as a human-machine system, is shown Fig. 1. In this loop, the driver is performing the control actions, guided by the advisor information. The advisor considers a reference to track, and driver-train state measurements. The driver is subject to behaviour variation due to exogenous factor. The non-intrusive sensors, i.e. detector, provide information from the driver to the advisor as an estimation of the current behaviour of the driver.

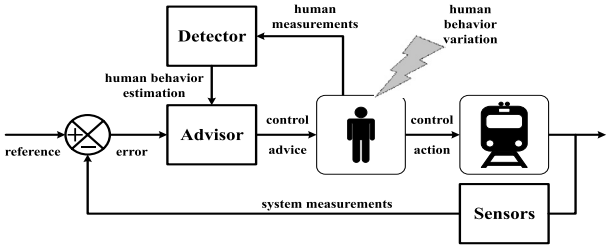

Fig. 1. General driver advisory control scheme

Train dynamics model: We considered the dynamics of the train modelled as a single-point mass subject to rolling mechanical resistance and aerodynamic drag. The running resistance, i.e. rolling mechanical resistance and aerodynamic drag of the train is given by Davis Formula, see Davis (1926).

$$k(v(t)) = k_0 + k_1 v(t) + k_2 v(t)^2, \tag{1}$$

where $v(t)$ is the train speed, the coefficients k_0, k_1, k_2 are real coefficients. They depend on the type of the train and can be obtained by wind tunnel test. The first two terms represent the rolling mechanical resistance, and the third term is the aerodynamic drag. In the current study, we are considering medium range speed, thus both the rolling mechanical resistance and aerodynamic drag are given importance. Thus, the dynamic equation of the motion of the train is considered as

$$m\dot{v}(t) = u(t) - mk(v(t)), \tag{2}$$

where, m is the lumped-mass of the train, $v(t)$ is the speed of the train (m/s), $k(v(t))$ is the running resistance to the motion and $u(t)$ is the traction/braking effort of the train. For cruise control of the train, we assumed that the train runs at a constant cruise speed, i.e. $v_r(t) \equiv v_r = const$.

Further, we let $e(t) = v(t) - v_r(t)$ and the driver control to maintain cruise speed as $u(t) = \hat{u}(t) + \bar{u}(t)$, with $\bar{u}(t)$ as the reference control necessary to maintain the cruise speed v_r and $\hat{u}(t)$ as the stabilizing/robust part of the control. Then, we can get the linearised error dynamical equation around the equilibrium state ($\dot{v}_r(t) = 0$) as,

$$\begin{aligned} m\dot{e}(t) = {} & \hat{u}(t) - mk_1 e(t) - 2mk_2 e(t) v_r \\ & + \bar{u}(t) - mk_0 - mk_1 v_r - mk_2 v_r^2. \end{aligned} \tag{3}$$

Thus, the error dynamical equation can be reformulated as,

$$\dot{e}(t) = Ae(t) + B\hat{u}(t) + B\bar{u}(t) - k_0 - k_1 v_r - k_2 v_r^2, \tag{4}$$

where, $A = -k_1 - 2k_2 v_r$, $B = 1/m$. In order to achieve the stabilisation of the high speed train at the cruise speed, the error dynamic equation is needed to be stabilised by a continuous-time driver controller. Next we will present driver model details.

Driver model: We choose the following driver control,

$$u(t) = \hat{u}(t) + \bar{u}(t), \text{ with } \hat{u}(t) = K(d(t))\eta(t), \tag{5}$$

where, $K(d(t))$ is the ability of the driver to interpret the advised control action $\eta(t)$. Here, we considered $K(d(t))$ to be time varying as it is observed that compared to the acceleration/braking phase, driver behaviour is prone to change during long cruise phases. The fatigue of long driving hours may result in poor judgement of appropriate control actions.

The variation of the behaviour (modelled here as $K(d(t))$) depends on various external driving conditions and also on the internal condition as physiological or psychological condition of driver. For the sake of simplicity, we consider $d(t)$ to be an external and measurable signal, which triggers the change of the driver behaviour. Specifically, We considered that $K(d(t))$ varies inside a polytope defined as,

$$K(d(t)) = K_{nom} + \Delta K d(t) \in Co\{K_1, K_2\}, \tag{6}$$

with $K_i \in \mathbb{R}^{1\times 1}$, $\forall i \in \{1,2\}$. Here, K_{nom} represents the nominal driver behaviour and $\Delta K = K_{max} - K_{nom}$ represent the difference between the nominal and the maximum ab-nominal driver behaviour. Here, we assume that $d(t)$ remains bounded and continuous for the cruising phase of the train.

Remark 1: Here, we considered a one dimensional proportional model for representing the driver behaviour and have not considered delay in driver response, as it helps in simplifying the short steps towards stability analysis of driver-train system.

The driver behaviour can potentially impact the performance of the train cruise control. Analytically, the variation can move the driver-train closed-loop system poles to negative half of s-plane. In order to compensate driver behaviour variation, we propose a sampled-data based neural-network controller.

2.2 Neural-network Controller

The input-output relationship of a TLFCFFNN is defined as,

$$Y_d(t_k) = \sum_{j=1}^{n_h} g_{d,j} t_f \left(\sum_{i=1}^{n} m_{j,i} X_i(t_k) + b_j \right), \; d \in \{1, \ldots, n_{out}\}, \tag{7}$$

where $m_{j,i}$, denotes the connection weight between the j^{th} hidden node and the i^{th} input node, $g_{d,j}$ denotes the connection weight between the d^{th} output node and the j^{th} hidden node, b_j

denotes the bias for the j^{th} hidden node, $t_f(.)$ denotes the activation function, n, n_{out} and n_h denotes the number of input, output and hidden nodes respectively, $X(t_k) = [X_1(t_k), \cdots, X_n(t_k)]^T$ denotes the sampled input vector X at the sampled time t_k. The structure of TLFCFFNN is as shown in Fig. 2.

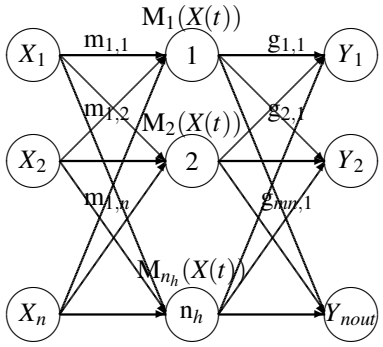

Fig. 2. TLFCFFNN-based controller

Thus, the sampled-data TLFCFFNN-based controller for the nonlinear system with $n_{out} = mn$ is defined as,

$$\eta(t) = \frac{\begin{bmatrix} Y_1(t_k) & Y_2(t_k) & \cdots & Y_n(t_k) \\ Y_{n+1}(t_k) & Y_{n+2}(t_k) & \cdots & Y_{2n}(t_k) \\ \vdots & \vdots & \ddots & \vdots \\ Y_{(m-1)n+1}(t_k) & Y_{(m-1)n+2}(t_k) & \cdots & Y_{mn}(t_k) \end{bmatrix} \begin{bmatrix} X_1(t_k) \\ X_2(t_k) \\ \vdots \\ X_n(t_k) \end{bmatrix}}{\sum_{l=1}^{n_h} t_f(\sum_{i=1}^{n} m_{l,i}X_i(t_k) + b_l)},$$

for all $t \in [t_k, t_{k+1})$, which can be further rewritten as

$$\eta(t) = \sum_{j=1}^{n_h} M_j(X(t_k))\mathbf{G}_j X(t_k), \tag{8}$$

$$\text{where,} \quad \mathbf{G}_j = \begin{bmatrix} g_{1,j} & g_{2,j} & \cdots & g_{n,j} \\ g_{n+1,j} & g_{n+2,j} & \cdots & g_{2n,j} \\ \vdots & \vdots & \ddots & \vdots \\ g_{(m-1)n+1,j} & g_{(m-1)n+2,j} & \cdots & g_{mn,j} \end{bmatrix}, \tag{9}$$

$$M_j(X(t_k)) = \frac{t_f(\sum_{i=1}^{n} m_{j,i}X_i(t_k) + b_j)}{\sum_{l=1}^{n_h} t_f(\sum_{i=1}^{n} m_{l,i}X_i(t_k) + b_l)} \in [0,1], \tag{10}$$

with the property $\sum_{j=1}^{n_h} M_j(X(t_k)) = 1$. It is assumed that the activation function $t_f(.)$ is chosen such that $t_f(\sum_{i=1}^{n} m_{j,i}X_i(t_k) + b_j) > 0$ and $\sum_{l=1}^{n_h} t_f(\sum_{i=1}^{n} m_{l,i}X_i(t_k) + b_l) \neq 0$ at any time to satisfy the property above.

Remark 2: Please note, that the expression of control given by equation (8) has $M_j(X(t_k))$ term, which acts as a scaling factor, due to the assumption $\sum_{j=1}^{n_h} M_j(X(t_k)) = 1$. The assumption also serves the purpose to bound the connection weight between input nodes and the hidden nodes, $m_{j,i}$ and the bias b_j with the help of activation function $t_f(.)$. The choice of activation function ensures that the value of $M_j(X(t_k))$ always lie between $[0,1]$. Thus, we consider boundedness of weights implicitly, contrary to work such as, Sahoo et al. (2016), where the authors consider the bounds on weights explicitly.

If we consider a simplified sampled-data based neural-network controller with $n_h = 2$ and the input vector of the neural-network as $X(t_k) = [X_1(t_k)\ X_2(t_k)]^T = [e(t_k)\ d(t_k)]^T$. Thus, the advisory control signal can be re written as,

$$\eta(t) = \sum_{j=1}^{n_h} M_j(X(t_k)) \left[G_{1,j}e(t_k) + G_{2,j}d(t_k)\right] \tag{11}$$

where, for $e(t_k),\ d(t_k) \in \mathbb{R}^1$ as one dimensioned, $G_{1,j}$ and $G_{2,j}$ will be $g_{1,j}$ and $g_{2,j}$ respectively, with the sampling instants $t_k,\ k \in \mathbb{N}$, that satisfy

$$t_0 = 0,\ 0 < t_{k+1} - t_k \leq h,\ \lim_{k\longrightarrow\infty} t_k = \infty. \tag{12}$$

Here, $e(t_k)$ and $d(t_k)$ are the speed error and driver behaviour measurements at t_k. While the aperiodic measurements of the speed can be due to sensor faults, the aperiodicity in driver behaviour measurements are mainly due to high computation time of embedded driver state estimation algorithms. So, at any instant, driver advisory system will only have time-delayed information of the state of driver-train system.

Remark 3: Note that the driver advisory control signal $\eta(t)$ is dependent on the time-delayed speed error and driver behaviour measurement. The task of advisory control is to compensate the driver varying behaviour, represented by $d(t)$, using appropriate $G_{1,j}$ and $G_{2,j}$ gain values.

2.3 Closed-loop System

The dynamic behaviour of the linearised continuous-time train system model with the driver and sampled-data based neural-network controller in closed-loop can be written as,

$$\dot{e}(t) = \sum_{j=1}^{n_h} M_j(X(t_k)) \Big[Ae(t) + BK(d(t))G_{1,j}e(t_k) + BK(d(t))G_{2,j}d(t_k) + B\bar{u}(t) - k_0 - k_1 v_r - k_2 v_r^2\Big]. \tag{13}$$

when $t_k \leq t < t_{k+1},\ k \in \mathbb{N}$. Further, if we assume that when driver behaves nominally, $d(t) = d_{nom}$, i.e. $d(t)$ is constant. Moreover, if during steady state, $\dot{e}(t) = 0$, $K(d(t)) = K(d_{nom}) = K_{nom}$ and $d(t) = d_{nom}$, we take the nominal driver control, $\bar{u}(t) = \sum_{j=1}^{n_h} M_j(X(t_k)) \left[B^{-1}(k_0 + k_1 v_r + k_2 v_r^2) - K_{nom}G_{2,j}d_{nom}\right]$. Thus the closed-loop equation can be given as,

$$\dot{e}(t) = \sum_{j=1}^{n_h} M_j(X(t_k)) \Big[Ae(t) + BK(d(t))G_{1,j}e(t_k) + BK(d(t))G_{2,j}w_1(t) + Bw_2(d(t))\Big]. \tag{14}$$

Here, if we consider $w_1(t) = d(t_k) - d_{nom}$ and $w_2(d(t)) = (K(d(t)) - K_{nom})G_{2,j}d_{nom}$, as small perturbations, corresponding to the measurement delays and deviation from the nominal performance respectively. The idea is to prove stability of the closed-loop system schematic as given in Fig. 3 and the closed-loop system equation as described by (14).

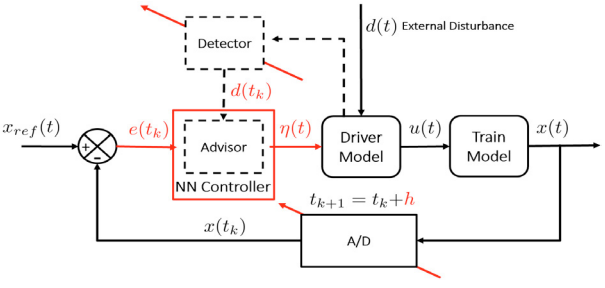

Fig. 3. Closed-loop system schematic

3. MAIN RESULT

3.1 System Description

In order to propose the theorem, we considered a general linearised continuous-time system described by

$$\dot{x}(t) = Ax(t) + Bu(t), \tag{15}$$

where $x = [x_1, \cdots, x_n]^T \in \mathbb{R}^n$ is the state vector and $u = [u_1, \cdots, u_m]^T \in \mathbb{R}^m$ denotes the control input vector. $A \in \mathbb{R}^{n\times n}$ and $B \in \mathbb{R}^{n\times m}$ are known constant system matrices, respectively and considered a sampled-data controller such that,

$$u(t) = \sum_{j=1}^{n_h} M_j(X(t_k)) \left[K(d(t))G_{1,j}x(t_k) + K(d(t))G_{2,j}d(t_k)\right]$$

where, $X(t_k) = [x(t_k)\, d(t_k)]^T$, $d(t) \in \mathbb{R}^r$, $G_{1,j} \in \mathbb{R}^{l\times n}$ and $G_{2,j} \in \mathbb{R}^{l\times r}$, $K(d(t)) \in Co\{K_1, \cdots, K_q\}$ with $K_i \in \mathbb{R}^{m\times l}$, $\forall i \in \{1, \cdots, q\}$, and the sampling instants t_k, $k \in \mathbb{N}$ satisfy

$$t_0 = 0,\ 0 < t_{k+1} - t_k \le h,\ \lim_{k\longrightarrow\infty} t_k = \infty. \tag{16}$$

Then, the closed-loop system can be written as,

$$\begin{cases} \dot{x}(t) = \sum_{j=1}^{n_h} M_j(X(t_k)) \Big[Ax(t) + BK(d(t))G_{1,j}x(t_k) \\ \qquad +BK(d(t))G_{2,j}w_1(t) + Bw_2(d(t))\Big], \\ z(t) = Cx(t), \end{cases} \tag{17}$$

when $t_k \le t < t_{k+1}$, $k \in \mathbb{N}$, with $w_1(t) = d(t_k) - d_{nom}$ and $w_2(d(t)) = (K(d(t)) - K_{nom})G_{2,j}d_{nom}$ as small perturbations.

Remark 4: Please note, we assume that the B matrix of the closed-loop system (17) is square and invertible. The assumption fits well for the driver advisory train control system design context and eases the computation of $\bar{u}(t)$.

Now that the system setup has been presented, we briefly recall L_2 stability notion before stating the main objective.

Definition 1: A linear system F is said to be finite-gain L_2-stable from w to Fw with an induced gain less than γ, if, F is a linear operator from L_2 to L_2 and if there exist positive real constants γ and η such that for all $w \in L_2$,

$$\|Fw\|_{L_2} \le \gamma\|w\|_{L_2} + \eta$$

Proposition: [Adapted from, Fridman (2010).]

Assume that there exist constants $\gamma_1 \ge 0$, $\gamma_2 \ge 0$ and a positive continuous function $V : t \in \mathbb{R}^+ \to V(t) \in \mathbb{R}^+$, differentiable for all $t \ne t_k$, $k \in \mathbb{N}$ that satisfy,

$$\dot{V}(t) + z^T(t)z(t) - \gamma_1 w_1^T(t)w_1(t) - \gamma_2 w_2^T(t)w_2(t) \le 0, \tag{18}$$

along the given closed-loop system. Then, the closed-loop system is L_2 stable from w_1 to z and w_2 to z with gain less than γ_1 and γ_2 respectively.

Proof: [Adapted from, Fridman (2010).]

Further, we will define Legendre polynomials, necessary for the stability proof.

Definition 2: The Legendre polynomials considered over the interval $s \in [a,b]$ and for $\forall k \in \mathbb{N}$ can be defined as,

$$L_k(s) = \sum_{l=0}^{k} p_l^k \left(\frac{s-a}{b-a}\right)^l \text{ with } p_l^k = (-1)^{l+k}\binom{k}{l}\binom{k+l}{l},$$

The polynomial function satisfies the following properties,

$$1)\ L_k(b) = 1,\ L_k(a) = (-1)^k, \tag{19}$$

$$2)\ \int_a^b L_k(s)L_l(s)ds = \begin{cases} 0 & \text{if } k \ne l, \\ \dfrac{b-a}{2k+1} & \text{if } k = l \end{cases}. \tag{20}$$

Further, we present some lemmas, necessary to obtain the proposed stability criteria.

Lemma 1: (Park and Park (2018)) For a non-negative integer N, let $x(s) \in \mathbb{R}^n$ be an integrable function: $\{x(s) \mid s \in [a,b]\}$. Then we have,

$$\int_a^b (s-a)^N x(r)dr = N!\mathbb{I}_N(a,b), \tag{21}$$

where, $\mathbb{I}_N(a,b) = \int_a^b \int_{s_1}^b \cdots \int_{s_N}^b x(s_{N+1})ds_{N+1}\cdots ds_1.$ (22)

Proof: [Adapted from, Lee et al. (2017).]

Lemma 2: Let $x(s) \mid s \in [a,b] \to \mathbb{R}^n$ be a continuous function. Then, for a non-negative integer N, a positive integer c, an arbitrary vector $\zeta \in \mathbb{R}^{cn}$, $R \in \mathbb{S}_+^n$, and a matrix $F \in \mathbb{R}^{cn\times(N+1)n}$ with appropriate dimensions, the following inequality holds:

$$-\int_a^b \dot{x}^T(s)R\dot{x}^T(s)ds \le (b-a)\zeta^T F R_N^{-1} F^T\zeta + \mathbf{He}\left\{\zeta^T F\mathbb{L}(a,b)\right\}, \tag{23}$$

where, $R_N = diag\{R, 3R, \cdots, (2N+1)R\}$ and $\mathbb{L}(a,b) = col\{\mathbb{L}_0(a,b), \cdots, \mathbb{L}_N(a,b)\}$ with $\mathbb{L}_k(a,b) =$

$$\begin{cases} x(b) - x(a) & \text{if } k = 0 \\ x(b) - (-1)^k x(a) - \sum_{l=1}^{k} p_l^k \dfrac{l!}{(b-a)^l}\mathbb{I}_{l-1}(a,b) & \text{for } k \in \mathbb{N} \end{cases} \tag{24}$$

Proof: [Adapted from, Lee et al. (2018).]

The main purpose of this paper is to guarantee the L_2-stability of the closed-loop linearised continuous-time train dynamical system with the driver and sampled-data based neural-network controller, (17). In addition, we are also interested in finding an estimation of the largest allowable sampling interval h, (12), for which L_2 stability is guaranteed.

3.2 Stability Analysis

We consider a Lyapunov-Krasovskii framework based approach to analyse the system's stability, Seuret and Gouaisbaut (2018). To this aim, we propose the LKF $V(t) = \sum_{i=1}^4 V_i(t) \forall t \in [t_k, t_{k+1})$ with

$$\begin{cases} V_1(t) \triangleq \bar{V}_1(t,x_t) = \eta_1(t)^T P\eta_1(t), \\ V_2(t) \triangleq \bar{V}_2(t,x_t) = \int_{t_k}^t \eta_2(t,s)^T Q\eta_2(t,s)ds, \\ V_3(t) \triangleq \bar{V}_3(t,\dot{x}_t) = (t_{k+1}-t)\int_{t_k}^t \dot{x}(s)^T Z\dot{x}(s)ds, \\ V_4(t) \triangleq \bar{V}_4(t,x_t) = (t_{k+1}-t)\begin{bmatrix} x(t) \\ x(t_k)\end{bmatrix}^T \Psi_0 \begin{bmatrix} x(t) \\ x(t_k)\end{bmatrix}, \end{cases} \tag{25}$$

with $\eta_1(t) = col\left\{x(t), x(t_k), \int_{t_k}^t x(s)ds, \frac{1}{t-t_k}\int_{t_k}^t\int_s^t x(r)drds\right\}$, $\eta_2(t,s) = col\left\{\dot{x}(s), x(s), x(t), x(t_k), \int_s^t x(r)dr\right\}$, and $P \in \mathbb{S}_+^{4n\times 4n}$, $Q \in \mathbb{S}_+^{5n\times 5n}$, $Z \in \mathbb{S}_+^n$ & X, $X_1 \in \mathbb{R}^{n\times n}$ are matrices to be determined.

Remark 5: The LKF terms are inspired from different papers. V_1, V_2 are inspired from Park and Park (2018), V_3 from Fridman (2010) and V_4 is similar to the one in Naghshtabrizi et al. (2008) and is also used in Fridman (2010). The contribution of this paper is to bring time-delay based functional to prove the L_2-stability of the closed-loop system (17).

Theorem 1. Consider scalar c, N, γ_1, γ_2, $h > 0$, and matrices $K_i \in \mathbb{R}^{m\times l}$, $i \in \{1, \cdots, q\}$, $G_{1,j} \in \mathbb{R}^{l\times n}, G_{2,j} \in \mathbb{R}^{l\times r}$, $j \in \{1, \cdots, n_h\}$. If there exist positive definite matrices $P \in \mathbb{S}_+^{4n\times 4n}$, $Q \in \mathbb{S}_+^{5n\times 5n}$, $Z \in \mathbb{S}_+^n$ and arbitrary matrices X, X_1, P_2, $P_3 \in \mathbb{R}^{n\times n}$, $F \in \mathbb{R}^{cn\times(N+1)n}$, $Y_k \in \mathbb{R}^{cn\times n} (k = 1,2)$ such that the following LMIs hold:

$$\begin{bmatrix} \Phi_h^{i,j} & \sqrt{h}F \\ * & -Z_N \end{bmatrix} \preccurlyeq 0 \tag{26}$$

$$\left[\Phi_0^{i,j} + he_7^T Ze_7 + h\mathbf{He}\left\{\rho_{\psi 0}^T \Psi_0 \rho_{\psi 1}\right\}\right] \preccurlyeq 0 \qquad (27)$$

for all $i \in \{1,\cdots,q\}$, and with $\Phi_{[t-t_k]}^{i,j} = \rho_{q0}^T Q \rho_{q0} - \rho_{\psi 0}^T \Psi_0 \rho_{\psi 0} + e_1^T C^T C e_1 - \gamma_1 e_8^T e_8 - \gamma_2 e_9^T e_9 + \mathbf{He}\left\{\rho_{p1}^T P \rho_{p2} + \rho_{q1}^T Q \rho_{q2} + F\rho_f + Y_1 \rho_{y1} + Y_2 \rho_{y2} + \left[e_1^T P_2^T + e_7^T P_3^T\right] \times \left[-e_7 + Ae_1 + BK_i G_{1,j} e_2 + BK_i G_{2,j} e_8 + Be_9\right]\right\}$, where,

$$\Psi_0 = \begin{bmatrix} \frac{X+X^T}{2} & -X+X_1 \\ * & -X_1 - X_1^T + \frac{X+X^T}{2} \end{bmatrix},$$

$$\begin{aligned}
\rho_{q0} &= col\{e_7, e_1, e_1, e_2, e_0\},\\
\rho_{\psi 0} &= col\{e_1, e_2\},\\
\rho_{\psi 1} &= col\{e_7, e_0\},\\
\rho_{p1} &= col\{e_1, e_2, e_5, e_6\},\\
\rho_{p2} &= col\{e_7, e_0, e_1, e_1 - e_4\},\\
\rho_{q1} &= col\{e_1 - e_2, e_5, (t-t_k)e_1, (t-t_k)e_2, (t-t_k)e_6\},\\
\rho_{q2} &= col\{e_0, e_0, e_7, e_0, e_1\},\\
\rho_f &= col\{e_1 - e_2, e_1 + e_2 - 2e_3, e_1 - e_2 + 6e_3 - 12e_4\},\\
\rho_{y1} &= col\{(t-t_k)e_3 - e_5\},\\
\rho_{y2} &= col\{(t-t_k)e_4 - e_6\},\\
e_i &= \left[0_{n\times(i-1)n}\ I_n\ 0_{n\times(c-i)n}\right],\ i = 1,\cdots,c,\\
e_0 &= \left[0_{n\times cn}\right],
\end{aligned}$$

then system (15) is L_2-stable from $w_1(t) \to z(t)$ and $w_2(d(t)) \to z(t)$ with L_2 gain less than γ_1 and γ_2 respectively.

Proof. Due to space restrictions, the proof is left to technical report, Jain et al. (2021).

4. NUMERICAL SIMULATIONS

In this section, numerical experiments are implemented to verify the effectiveness of neurel-network based driver advisory train cruise control system to reduce the tracking error in the presence of varying behaviour of the driver. The parameters m, k_0, k_1, and k_2 of the train are considered as $800 \times 10^3 kg$, $0.01176N/kg$, $0.00077616N\,s/m\,kg$ and $1.6 \times 10^{-5} N\,s^2/m^2\,kg$ respectively, and are chosen from the experimental results of Japan Shinkansen train, Maeda et al. (1989). We consider a situation where the driver must accelerate the train speed from 220km/h to 240km/h and then maintain the cruise speed as:

$$v_r(t) = \begin{cases} 220 \text{ km/h}, & \text{if } 0s \le t < 1500s, \\ 240 \text{ km/h}, & \text{if } 1500s \le t < 12000s, \end{cases} \qquad (28)$$

Such scenarios of increasing/decreasing the cruise speed are very common. During the train journey, the driver advisory system provide graphical/text advice about the train current speed and also about train target speed. Generally, the change in target speed signal depends on the track clearance. The driver has to react to this target speed update, with a nominal expected behaviour and apply the control $u(t)$ given by (5), to stabilise the error dynamics given by (4).

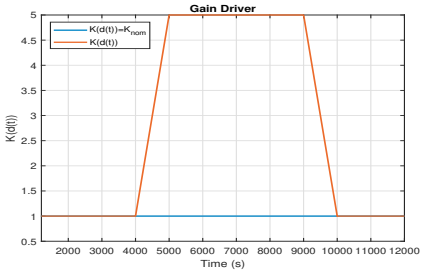

Fig. 4. The nominal K_{nom} and varying $K(d(t))$ driver state

During simulation, driver's state, which is related to his attention/vigilance state, varies according to equation (6). Here, t_{dstart} and t_{dend} are the time when the decay starts and when it ends, and T_{decay} is the time needed to decay from nominal K_{nom} to maximum ab-nominal driver K_{max} behaviour. Fig. 4 shows the modelled variation of the driver behaviour. In order to obtain this variation, we considered $t_{dstart} = 4000s$, $t_{dend} = 10000s$ $K_{nom} = 1$, $K_{max} = 5$, and $T_{decay} = 1000s$. On top of driver's related disturbance, we are considering a wind gust disturbance acting on the train. The wind disturbance is assumed to last during the interval $[t_{dstart}, t_{dend}]$ as

$$w(t) = \begin{cases} 0.002\sin(0.01t) & if\ t_{dstart} < t < t_{dend} \\ 0 \text{ otherwise.} \end{cases} \qquad (29)$$

We now consider the following two cases for a NN with $t_f(.) = \frac{1}{1+exp\left(-\sum_{i=1}^{n_x} m_{j,i} x_i(t_k) - b_j\right)}$, with $b_j = 0$, $\forall j \in \{1,\cdots,n_h\}$.

Case 1: Advisory control with delayed speed measurements.
In this case, when driver is inattentive (variation of the gain $K(d(t))$), advisory control is not aware of driver's state variation, so the signal $\eta(t)$ given by (11), is only based on tracking error, i.e. $\eta(t) = \sum_{j=1}^{n_h} M_j(X(t_k)) G_{1,j} e(t_k)$. Note, here $G_{2,j} = 0$, $\forall j \in 1,\cdots,n_h$. In our recent paper, Jain et al. (2020b), for the similar scenario, we presented stability result with a sampled-data based state-feedback controller. The state-feedback controller given by LMIs in Jain et al. (2020b) was unstable beyond delay of $h = 285s$. Here, we aim to compare both these results to highlight performance improvement by use of neural-network based driver advisory train cruise control. For this scenario, Fig. 5 presents comparison of speed $v(t)$ response for these two controllers. In order to simulate this case, we considered $m_{1,1}$, $m_{1,2}$, $m_{2,1}$, $m_{2,2} = 0.5$ and $G_{1,1}$, $G_{1,2} = -0.75$ and $G_{2,1}$, $G_{2,2} = 0$. We can observe that neural-network based driver advisory control signal generator performs better even at the maximum delay limit performance for a sampled-data based state-feedback driver advisory train cruise control.

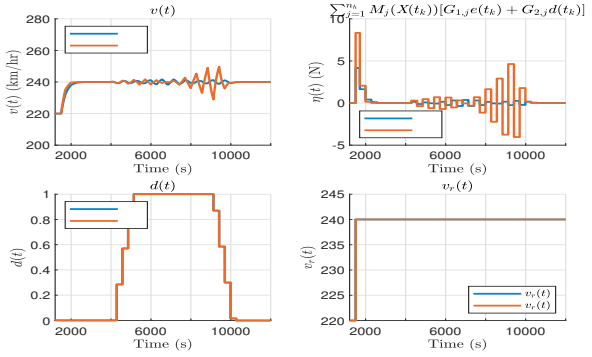

Fig. 5. The response of $v(t)$, $\eta(t)$ and $d(t)$ with sampled-data based (red) and neural-network based (blue) based ADAS assistance to varying driver behaviour in the presence of train speed measurements only

Case 2: Advisory control based on both delayed speed and driver behaviour measurements.
In this case, when driver is inattentive, advisory control uses both time-delayed train speed, $e(t_k$ and driver state $d(t_k)$ measurements for advisory train control signal $\eta(t)$ given by (11). In order to simulate this case, we considered $m_{1,1}$, $m_{1,2}$, $m_{2,1}$, $m_{2,2} = 0.5$ and $G_{1,1}$, $G_{1,2} = -0.75$ and $G_{2,1}$, $G_{2,2} = -1$. Again, we compared results with sampled-

data state-feedback based driver advisory train controller of Jain et al. (2020b) with the current controller. Fig. 6 gives speed $v(t)$ response for this scenario. In Jain et al. (2020b), the maximum limit for delayed driver and train state measurement was found to be around $h = 245s$. Beyond this limit, the closed-loop system was unstable. The response even degraded at this limit. The first point that We can notice from Fig. 6 is that, when the train speed and the driver state measurements are both considered, the cruise speed is decreased during the time when driver is inattentive (safety control). Further, now if we compare response of sampled-data based state-feedback and neural-network driver advisory train control, the later outperforms the former at the maximum delay of Jain et al. (2020b). This signifies that neural-network based driver advisory train cruise control is reducing the cruise speed in the form of a steady state error, while maintaining the train stability. The h limit that satisfy LMIs given by (26) and (27) for stability is larger than that found in Jain et al. (2020b). Thus we can positively argue that, neural-network based driver advisory train control system can allow (because of its inherent non-linearity) a larger time-delay in driver state measurement to decide driver advisory signal while ensuring train stability.

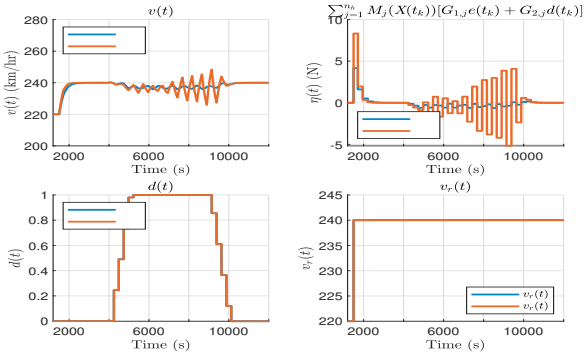

Fig. 6. The response of $v(t)$, $\eta(t)$ and $d(t)$ with sampled-data based (red) and neural-network based (blue) based ADAS assistance to varying driver behaviour in the presence of both train speed and driver state measurements

5. CONCLUSION

In this paper, we developed L_2 stability sufficient conditions for non-linear aperiodically sampled systems. In particular, the NNCDIL application was investigated, with a neural-network controller in series with a human driving a train. The stability conditions were derived in LMI form, using augemented LKF and Bessel-Legendre inequality by adapting the time-varying delay results to aperiodical sampling context. Using the derived conditions, it is also possible to estimate the maximum acceptable sampling delay, and use this information to avoid instability for real applications. The implications of our results are twofold : First-of-all, we developed a framework to assess stability of approximate computing solutions for advisory control, where neural-networks are use to approximate and replace exogenous devices for embedded architectures. Secondly, we propose a control-theoretic approach to assess stability of Human Machine Systems, that suffer from modelling and measurement uncertainties. The proposed approach is able to interpret these uncertainties quantitatively and use them for advisory controller design with guaranteed performance. This makes the certification process of advanced driver assistance systems easier by using advanced control techniques such as model based control and neural-networks. The perspectives of this research are in the extension of the results for other types of NNC such as Recurrent Neural Networks, or more refined driver models or by considering Human-Machine shared control of transportation systems.

REFERENCES

Chen, S. and Wen, J.T. (2019). Industrial robot trajectory tracking using multi-layer neural networks trained by iterative learning control. *arXiv preprint arXiv:1903.00082*.

Davis, W.J. (1926). The tractive resistance of electric locomotives and cars. *General Electric Review*, 29(10), 685–707.

Fridman, E. (2010). A refined input delay approach to sampled data control. *Automatica*, 46(2), 421–427.

Jain, A.K., Berdjag, D., Fiter, C., and Polet, P. (2021). Technical report on stability of neural-network based train cruise advisory control systems with aperiodically measurements. In *https://drive.google.com/file/d/1ZMuEa8v-gOCSfF64rojZoGz8ib2Yb$_q$x/view?usp = sharing*.

Jain, A.K., Fiter, C., Berdjag, D., and Polet, P. (2020a). Exponential stability criteria for neural network based control of nonlinear systems. In *IEEE ACC*, 1631–1636.

Jain, A.K., Fiter, C., Berdjag, D., and Polet, P. (2020b). Investigating stability for driver advisory train cruise control systems with aperiodic measurements. In *IEEE ITSC*, 1–6.

Jain, A.K., Fiter, C., Berdjag, D., Polet, P., and Béarée, R. (2019). Approximate computing control approaches using recurrent neural networks. In *JN-JDMACS*, 1–4.

Lee, S.Y., Lee, W.I., and Park, P. (2017). Polynomials-based integral inequality for stability analysis of linear systems with time-varying delays. *JFKI*, 354(4), 2053–2067.

Lee, S.Y., Lee, W.I., and Park, P. (2018). Orthogonal-polynomials-based integral inequality and its applications to systems with additive time-varying delays. *JFKI*, 355(1).

Maeda, T., Kinoshita, M., Kajiyama, H., and Tanemoto, K. (1989). Aerodynamic drag of shinkansen electric cars. *Railway Technical Research Institute, Quaterly Reports*, 30(1).

Miglianico, D., Vanderhaegen, F., Polet, P., Mouchel, M., Dahyot, R., and Berdjag, D. (2018). Ep3375690a1 : Driving assistance method for a railway vehicle and a railway vehicle supervision system. *European Patent Office*.

Mittal, S. (2016). A survey of techniques for approximate computing. *ACM Computing Surveys (CSUR)*, 48(4), 1–33.

Naghshtabrizi, P., Hespanha, J.P., and Teel, A.R. (2008). Exponential stability of impulsive systems with application to uncertain sampled data systems. *Systems & Control Letters*.

Park, J. and Park, P. (2018). Stability analysis for systems with time-varying delay via orthogonal-polynomial-based integral inequality. *IFAC-PapersOnLine*, 51(14), 277–281.

Sahoo, A., Xu, H., and Jagannathan, S. (2016). Neural network based event triggered state feedback control of nonlinear continuous time systems. *IEEE TNNLS*, 27(3), 497–509.

Seuret, A. and Gouaisbaut, F. (2018). Stability of linear systems with time-varying delays using bessel–legendre inequalities. *IEEE TAC*, 63(1), 225–232.

Sikander, G. and Anwar, S. (2019). Driver fatigue detection systems: A review. *IEEE ITSC*, 20(6), 2339–2352.

Sommer, D. and Golz, M. (2010). Evaluation of perclos based current fatigue monitoring technologies. In *IEEE Engineering in Medicine and Biology*, 4456–4459.

Zhang, X.M., Han, Q.L., Seuret, A., Gouaisbaut, F., and He, Y. (2018). Overview of recent advances in stability of linear systems with time-varying delays. *IET Control Theory & Applications*, 13(1), 1–16.